INSTITUTE OF PHYSICS PUBLISHING JOURNAL OF PHYSICS D: APPLIED PHYSICS

J. Phys. D: Appl. Phys. **37** (2004) 898–906 PII: S0022-3727(04)71550-8

Detecting solid–liquid interface properties with mechanical slip modelling for quartz crystal microbalance operating in liquid

F Lu[1], H P Lee[1,2,3] and S P Lim[1]

[1] Department of Mechanical Engineering, National University of Singapore, 9 Engineering Drive 1, 117576, Singapore

[2] Institute of High Performance Computing, 1 Science Park Road, #01-01 The Capricorn, Singapore Science Park II, 117528, Singapore

E-mail: hplee@ihpc.a-star.edu.sg

Received 7 November 2003
Published 24 February 2004
Online at stacks.iop.org/JPhysD/37/898 (DOI: 10.1088/0022-3727/37/6/014)

Abstract

Quartz crystal microbalances (QCMs) provide sensitive probes for changes at solid–solid or solid–liquid interfaces. It is essential to obtain a physical insight into the details of the interface loading mechanism to interpret the observed behaviour leading to fresh applications of AT-cut quartz resonators. In this work, a mechanical slip model of the interface between a quartz plate and a viscoelastic liquid is presented to replace the continuous displacement assumption. The electrical impedance of a compounded quartz crystal resonator is expressed as a function of the properties of liquid, and the quartz and the strength of contact attraction between the solid and liquid. The interfacial slip parameter between the solid and liquid, which is defined as the displacement transmission from solid particles to liquid bottom particles, is explicitly calculated from the complex attraction strength between the liquid and solid. Comparisons of the physical slip model with other interfacial modes used in the QCM are presented, including the continuous mode and the transmission mode based on the friction force interface. The explicit expression of the slip parameter is presented, and the influence of interfacial slip on QCM measurements is discussed with numerical results. A detailed physical description of the solid–liquid interfacial is useful for exploring fresh ideas for the use of the QCM in biological industry. A new approach by using the slip parameter measured with QCM is proposed to determine the attraction strength between the particles of a viscous liquid and solid particles. The experimental data in the literatures for a hydrophilic-coated sensor and a hydrophobic-coated sensor are used for the numerical examples. It is found that the imaginary part of the interactive strength of these two types of sensor is almost the same. The real part of the interactive strength contributes significantly to distinguish the different interface conditions for these two types of sensor.

1. Introduction

Quartz crystal microbalances (QCMs) provide a simple and effective means for detecting changes in the physical properties of thin layers at their surfaces. Sauerbrey [1] first reported a linear relationship between the resonance frequency of the AT-cut quartz crystal and the mass of the film attached to its surface. The Sauerbrey equation is valid under the condition that the film is rigid and it is rigidly coupled to the oscillatory motion of the quartz crystal surface. One of the advantages of AT-cut QCMs is their ability to act as a chemical detector in a liquid environment. After the discovery that the QCM

[3] Author to whom any correspondence should be addressed.

resonator could also be used as a deposition monitor in liquids by Nomura [2], the application of the QCM has been extended into the complex liquid environment, including *in situ* monitoring as chemical and biological sensors [3, 4]. Many studies were devoted to the behaviours of QCMs under liquid loading. When a QCM operates in a liquid environment, the oscillation of the device's surface is coupled to the liquid. There is damping of the resonance of the QCM besides a resonance frequency shift. The molecular layer attached to the QCM surfaces is neither rigidly coupled nor is it that of a simple Newtonian liquid. To understand the resonance characteristics of QCMs in liquid environments and use it in biological measurement, development of models of the acoustic device response to the viscoelastic medium is essentially required.

A general approach to describing the performance of QCMs in liquid is to consider the acoustic impedance of the devices with interface acoustic impedance loading. This surface impedance summarizes the overall acoustic load acting on the quartz surface and can be easily applied to multiple viscoelastic layer arrangements [5]. With some approximations, this model is translated into electrical analogue approaches [6], which have served effectively as methods for electrically characterizing the crystal. However, the analogue method often masks the physical insight into the detailed nature of the loading mechanism. An alternative approach is based on a mechanical description so as to solve a set of acoustic wave equations of the compounded QCM. The first acoustic-wave analysis of a loaded resonator with an elastic overlayer was performed by Miller and Bolef [7] and then simplified by Lu and Lewis [8]. Reed *et al* [9] derived the electrical admittance of the QCM with a viscoelastic medium directly in terms of the physical properties of the compound resonator. Kanazawa [10] summarized the mechanical properties of the QCM and overlayer, correlating them with the observed electrical behaviours. A common feature of these treatments is that continuous shear stress and continuous displacement are assumed for the contact interface between the attached layer and sensor surface. The details of the contact interface are completely neglected, such as surface roughness, interface viscosity and interface slip.

The role of interfacial slip between the sensor surface and the attached medium is one of the many controversies in modelling in the QCM liquid environment. Ferrante [11] defined the slip parameter as the ratio of the displacements of the liquid bottom surface and the displacement sensor contact surface and employed it to replace the continuous displacement assumption as the boundary condition for solving the equations. The slip parameter was characterized by experiments. Rodahl and Kasemo [12] proposed that slip at the device interface could be related to the shear stress acting on the substrate due to the liquid. McHale [13] employed the slip friction law, which is proportional to the relative velocity between the contact surfaces, in the acoustic impedance analysis of acoustic wave sensors with multiple viscoelastic layers.

In an early paper [14], a mechanical slip modelling of the interface between a liquid and quartz plate has been proposed to analyse the performance of a QCM in liquid. The continuous displacement and stress assumption boundary conditions are replaced by the equations of motion of contact molecules. In this paper, the theoretical analysis of the interface slip model of a QCM in liquid is reviewed first. The electrical impedance of a compounded QCM is expressed in terms of the contact interface properties between solid and liquid, such as attraction strength, contact molecular size and viscosity of the host liquid. The slip parameter is expressed explicitly as functions of the interface attraction strength of the contact layers, G^*, and the viscosity of the liquid. Correlations between this mechanical slip model and other slip models are presented. The detailed mechanical description of the solid–liquid interface of a QCM in a liquid provides a physical approach to understanding the performance of a QCM in a liquid. With the mechanical slip model of the interface, a new approach using the slip parameter measured with a QCM is proposed to determine the attraction strength between the particles of a viscous liquid and solid particles. Experimental data in the literature for a hydrophilic-coated sensor and a hydrophobic-coated sensor are used for the numerical examples.

2. Theoretical modelling for analysis

2.1. Interface slip model for a QCM with a surface liquid layer

A QCM consists of a thin disc of an AT-cut quartz crystal plate with metal electrodes deposited on both surfaces. With perturbation of the mechanical load on the quartz surface, the resonance characteristics of the crystal refer primarily to the resonance frequency, and the quality factor will be changed following a certain relationship. A modified geometry of the one-dimensional analysis modelling of the compounded QCM is shown schematically in figure 1. The electrodes are assumed to be highly conducting, but with negligible thickness. Only the thickness shear displacement is considered, and the thickness shear displacement on the quartz surface is assumed to be uniform along the surface [15].

To evaluate the acoustic impedance exerted on the surface of the quartz plate by the layers compounded on its surface and the coupling effect of the quartz plate and the surface layers, it is necessary to solve a set of differential equations, including equations of piezoelectricity, the thickness shear wave equation of the quartz plate, and fluid motion equations for a viscous and incompressible fluid are summarized as follows [10]:

$$\rho_{\mathrm{q}}\ddot{u}_{\mathrm{q}} = \hat{c}_{\mathrm{q}}\frac{\partial^2 u_{\mathrm{q}}}{\partial y^2} \qquad \text{(TS wave equation for quartz plate)} \tag{1}$$

$$e_{26}\frac{\partial^2 u_{\mathrm{q}}}{\partial y^2} - \epsilon_{22}\frac{\partial^2 \phi}{\partial y^2} = 0$$
(piezoelectric coupling equation for quartz plate) (2)

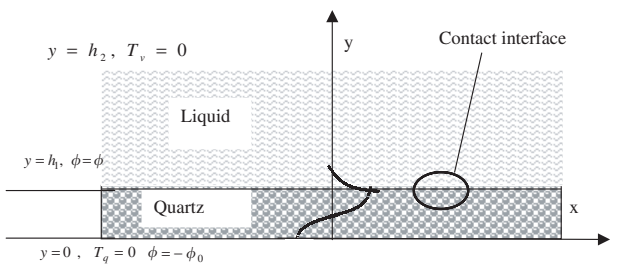

Figure 1. The schematic of the compounded QCM with a viscoelastic liquid.

A similar shear wave equation for the viscoelastic overlay can be expressed as

$$\rho_l \ddot{u}_l = \hat{c}_l \frac{\partial^2 u_l}{\partial y^2} \qquad \text{(TS wave equation in liquid layer)} \tag{3}$$

where u_q and u_l are the shear displacement of the quartz plate and liquid, which are functions of the coordinate y and time t, ρ_q, ρ_l are the density of the quartz and liquid, e_{26} is the appropriate piezoelectric constant of AT-cut quartz, ϵ_{22} is the permittivity of the quartz crystal, $\hat{c}_q = c_{66} + e_{26}/\epsilon_{22} + j\omega\eta_q$, with c_{66} the shear modulus and η_q the fictitious viscosity of quartz, and $\hat{c}_l = \mu_l + j\omega\eta_l$ with μ_l the shear modulus of the liquid and η_l its viscosity.

By assuming that shear displacements are harmonic functions of time with angular frequency ω, the general solutions for the quartz plate and fluid medium can be expressed as

$$u_q = [A_1 e^{-jk_q y} + B_1 e^{jk_q y}]e^{j\omega t} \tag{4}$$

$$u_l = [A_2 e^{-jk_v y} + B_2 e^{jk_v y}]e^{j\omega t} \tag{5}$$

where A_1, B_1, A_2, B_2 are constants to be determined by the boundary conditions, k_q and k_v are complex wavenumbers in terms of the shearing displacement of the quartz plate and fluid medium, respectively, which can be expressed as

$$k_q = \omega\sqrt{\frac{\rho_q}{\hat{c}_q}} \qquad \text{and} \qquad k_v = \omega\sqrt{\frac{\rho_l}{\hat{c}_l}} \tag{6}$$

The general solution for the electrical potential, ϕ, can be obtained by integrating equation (2) and is expressed as

$$\phi = \frac{e_{26}}{\epsilon_{33}} u_q + Cy + D \tag{7}$$

When QCM operates in the liquid environment, the oscillation of the quartz plate surface is coupled to the liquid and induces an oscillation in the liquid. The decay length of the shear wave in the viscous liquid is $\delta = (2\eta_l/\omega\rho_l)^{1/2}$, which is small when the liquid has a small viscosity and the frequency, ω, is moderate. For water, the decay length is of the order of 2400 Å. Accordingly, the shearing displacement, u_l, is damped out at a very short distance from the lower boundary and the effect of the wave reflection from the upper surface of the liquid layer becomes insignificant as long as $h_l/\delta \gg 1$. In that case, since there is no reflection from the fluid–air interface, the constant, A_2, of the positive exponential term on the liquid shearing displacement in equation (5) is equal to zero.

In order to solve the equations of motion with six unknown constants, six boundary conditions are needed. As shown in figure 1, the boundary conditions include a stress free boundary at the plate bottom surface (solid–air interface), zero shear displacement at the liquid top surface (liquid–air interface), potential boundaries on both quartz plate surfaces and the interface slip boundary conditions between the solid and the liquid interface at the bottom of the liquid layer. The stress free boundary at the plate bottom surface (solid–air interface), zero shear displacement at liquid top surface (liquid–air interface) and potential boundaries can be expressed as follows:

$$y = h_2,\ T_v = 0 \ \Rightarrow\ A_2 e^{jk_v h_2} - B_2 e^{-jk_v h_2} = 0 \tag{8}$$

$$y = h_1,\ \phi(h_1) = \phi_0 \ \Rightarrow\ \frac{e_{26}}{\epsilon_{22}}(A_1 e^{jk_q h_1} + B_1 e^{-jk_q h_1}) + h_1 C + D = \phi_0 \tag{9}$$

$$y = 0,\ T_q(h_1) = 0 \ \Rightarrow\ j\hat{c}_q k_q (A_1 - B_1) + e_{26} C = 0 \tag{10}$$

$$y = 0,\ \phi(h_1) = -\phi_0 \ \Rightarrow\ \frac{e_{26}}{\epsilon_{22}}(A_1 + B_1) + D = -\phi_0 \tag{11}$$

where h_1 and h_2 are the thickness of the quartz plate and the liquid layer, respectively, and ϕ_0 is the electrical potential on the quartz surface. Another two boundary conditions can be determined from the solid–liquid interface as shown in figure 2. At the interface between the quartz crystal surface and the viscoelastic molecular layer, the transverse vibratory motion of particles at the top of the crystal surface causes transverse motion of the particles of the attached layer in contact with the sensor surface. The transverse shear wave is partially transmitted and partially reflected. The amount of transmission and reflection depends on the physical and chemical properties of the interface and attached viscoelastic layers. The continuous displacement and stress assumptions mask the detailed mechanical behaviours of the contact interface.

The interfacial slip between the quartz surface and layer is modelled as a local molecular mass and interaction element between the masses as shown in figure 2, which has been proposed in an early paper [14]. m_1 represents the mass of a particle on the layer surface, and m_2 represents the mass of a particle on the quartz surface. Displacements of both particles are restricted in the x-direction. The interaction between the two particles is presented as a spring and damper with complex parameter G^*, which is the force when a unit shear displacement occurs between two contacting particles. Besides the interaction force from the sensor surface particles, there is an internal attraction force from the bulk liquid. The interaction is proportional to the gradient of the displacement in the x-direction. The interaction force between the two contacting surfaces molecules is modelled as a spring–dashpot force that is proportional to the relative displacement/velocity between the molecules of the two surfaces. The shear force on the interface is equal to the spring force plus the damping force.

The lateral displacement of the quartz contact surface molecules is noted as u_q^h, and the displacement of the particles

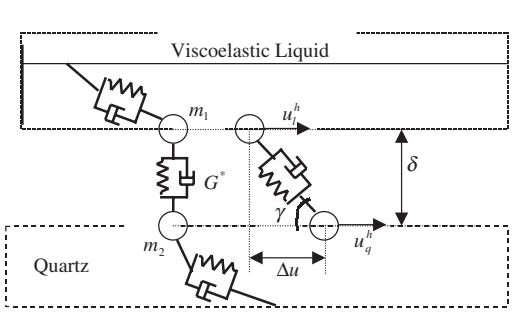

Figure 2. Mechanical slip model of the contact solid–liquid interface.

of contact at the liquid bottom is denoted as u_1^h. The relative displacement in the x-direction can be expressed as $\Delta u = u_q^h - u_1^h$. The attractive force is proportional to the relative shear displacement. This assumption is valid when the relative deformation is small, which is within the linear elastic region. The equivalent shear force of the interface can be expressed as

$$T_b = G^*\gamma = \frac{G^*}{\delta}(u_q^h - u_1^h) \tag{12}$$

where δ is the distance between the molecules on the quartz surface and those on the viscoelastic layer contact surface as illustrated in figure 2. The force keeping the connection between the two contact surfaces is like the shear stress on the continuous medium. The single shear vibration mode is considered in the QCM compound resonator; the particles on the surface have the same vibration phase. Based on the equations of motion for particles on both the viscoelastic layer and the top of quartz plate, another two boundary conditions on the interface between the liquid and solid can be expressed as [14]

$$\frac{G^*}{\delta}e^{jk_qh_1}A_1 + \frac{G^*}{\delta}e^{-jk_qh_1}B_1 + \left[-\rho_l\Delta_l\omega^2 + j\hat{c}_lk_v - \frac{G^*}{\delta}\right] \times e^{jk_vh_1}A_2 + \left[-\rho_l\Delta_l\omega^2 - j\hat{c}_lk_v - \frac{G^*}{\delta}\right]e^{-jk_vh_1}B_2 = 0 \tag{13}$$

$$\left[-\rho_q\Delta_q\omega^2 + j\hat{c}_qk_q + \frac{G^*}{\delta}\right]e^{jk_qh_1}A_1 + \left[-\rho_q\Delta_q\omega^2 - j\hat{c}_qk_q + \frac{G^*}{\delta}\right]e^{-jk_qh_1}B_1 + e_{26}C = \frac{G^*}{\delta}e^{jk_vh_1}A_2 + \frac{G^*}{\delta}e^{-jk_vh_1}B_2 \tag{14}$$

where Δ_q and Δ_l are the particle thickness of the quartz contact layer and liquid layer, respectively, and $G^* = G' + j\omega G''$ is the complex attraction parameter of the contact interface. The continuous displacement assumption and continuous stress assumption on the interface are replaced by a more detailed description of the contact interfacial properties. Constants A_1, B_1, A_2, B_2, C, D can be solved based on the six equations (8)–(11), (13) and (14).

2.2. Electrical impedance of the compounded QCM in liquid

The wave displacement generates an accompanying electrical potential through which the piezoelectric wave can be electrically detected. Impedance/admittance analysis, in which the spectrum of the impedance/admittance of the compound sensor is recorded as a function of the excitation frequency, is widely used to detect the perturbation on the BAW sensors. The admittance is defined as the ratio of the input current and voltage. The explicit expression of the current of the piezoelectric materials is $Q = \int_{\bar{A}} D_2\,dA$ [9]. The current across the quartz crystal, which is the time derivative of the charge, can be expressed as

$$I = -j\omega\epsilon_{22}C\bar{A} \tag{15}$$

where $\bar{A}$ is the effective electrode surface area and C is the constant from equation (7). The admittance of quartz crystal resonator can be determined as

$$Z = \frac{V}{I} = \frac{2\phi_0}{j\omega\epsilon_{22}\bar{A}}\frac{1}{C} \tag{16}$$

After the constant C is determined from the boundary conditions, the spectrum of the admittance can be predicted.

Substituting the constant determined from boundary conditions into equation (16), the corresponding impedance of the compounded QCM with a viscoelastic layer based on mechanical slip interface modelling can be expressed as

$$Z = \frac{V}{I} = \left[(e_{26}^2a_1 - h_1\epsilon_{22}a_5 - e_{26}^2)ls2 + \left(e_{26}^2\frac{1}{a_1} + h_1\epsilon_{22}a_5 - e_{26}^2\right)ls1\right] \times [j\omega\epsilon_{22}^2\bar{A}a_5(ls1 - ls2)]^{-1} \tag{17}$$

where

$$ls1 = a_1^2(a_2^2 + a_3^2)\left[\left(a_5 - a_{10} - \frac{a_5}{a_1}\right)(a_{11} + a_8) + a_8a_{11}\right] + a_1^2a_6(a_2^2 - a_3^2)\left(a_{10} - a_5 - a_8 + \frac{a_5}{a_1}\right)$$

$$ls2 = (a_2^2 + a_3^2)[(a_5 + a_{10} - a_1a_5)(a_{11} + a_8) - a_8a_{11}] + a_6(a_2^2 - a_3^2)(-a_{10} - a_5 + a_8 + a_1a_5)$$

$$a_1 = e^{jk_qh_1}, \qquad a_2 = e^{jk_vh_1}$$
$$a_3 = e^{jk_vh_2}, \qquad a_5 = j\hat{c}_qk_q \tag{18}$$
$$a_6 = j\hat{c}_lk_v, \qquad a_8 = \frac{G^*}{\delta}$$
$$a_{10} = \rho_q\Delta_q\omega^2, \qquad a_{11} = \rho_l\Delta_l\omega^2 \tag{19}$$

and $\bar{A}$ is the equivalent electrode surface on the quartz plate. Equation (17) is the general expression of the electrical impedance of a QCM with a viscoelastic overlayer on the surface with consideration of the mechanical slip on the solid–liquid interface. With certain assumptions, the expression can be simplified and compared with the earlier results.

2.3. Unperturbed quartz resonator—with zero attraction strength assumption

When the attractive strength between solid–liquid interfaces is equal to zero, i.e. there is no interactive couple between liquid and solid, the QCM works in the condition without any overlayer. Substituting attraction strength, $G^* = 0$, into equation (17) and neglecting the mass inertial exposure of the surface particles to the air, i.e. $a_8 = 0$ and $a_{10} = 0$, the electrical impedance of the unperturbed QCM can be expressed as

$$Z_m = \frac{e_{26}^2}{\hat{c}_qk_q\epsilon_{22}^2\omega\bar{A}}\frac{e^{jk_qh_1} - 1}{1 + e^{jk_qh_1}} - j\frac{h_1}{\epsilon_{22}\bar{A}\omega} = j\frac{e_{26}^2}{\hat{c}_qk_q\epsilon_{22}^2\omega\bar{A}}\tan\left(\frac{k_qh_1}{2}\right) - j\frac{h_1}{\epsilon_{22}\bar{A}\omega} \tag{20}$$

The zero of the electrical impedance of the unperturbed QCM appears when

$$\tan\left(\frac{k_qh_1}{2}\right) = \frac{\epsilon_{22}h_1\hat{c}_qk_q}{e_{26}^2} \tag{21}$$

which gives the series resonant frequency of the AT-cut quartz crystal resonator with first shearing mode vibration. The result derived from the mechanical model is the same as that derived from transmission line modelling [6].

2.4. Continuous displacement assumption with viscoelastic liquid—infinite attraction strength assumption

When the interfacial attraction strength is infinitely large, there is no slip between two contact interfaces. By neglecting the mass inertia of the contacting particles, the continuous displacement assumption at the solid–liquid interface is recalled and the results derived by Reed [9] and Kanazawa [10] can be reproduced. When the QCM is immersed into a liquid and the liquid depth is much larger than the decay length of the shearing wave, the QCM with infinite liquid coating can be obtained by setting $a_2 \gg a_3$. The electrical impedance of the QCM can be expressed as a function of the properties of the compounded liquid for QCM operating in half infinite bulk liquid as follows:

$$ls1 = a_1^2 a_5 - a_5 a_1 + a_1^2 a_6 \tag{22}$$

$$ls2 = a_5 - a_1 a_5 - a_6 \tag{23}$$

$$Z = \frac{V}{I} = \left[(e_{26}^2 a_1 - h_1 \epsilon_{22} a_5 - e_{26}^2) ls2 + \left(e_{26}^2 \frac{1}{a_1} + h_1 \epsilon_{22} a_5 - e_{26}^2 \right) ls1 \right] \times [\mathrm{j}\omega \epsilon_{22}^2 \bar{A} a_5 (ls1 - ls2)]^{-1} \tag{24}$$

2.5. Slip parameter for the compounded QCM in a viscoelastic liquid

The ratio between the complex displacement of the bottom particles of the liquid and the displacement of the sensor surface displacement is defined as the slip parameter by Ferrante [11].

$$\alpha = \frac{u_1^{\mathrm{h}}}{u_{\mathrm{q}}^{\mathrm{h}}} \tag{25}$$

Based on the mechanical slip modelling of the interface, the slip parameter can be expressed as

$$\alpha = \frac{A_2 \mathrm{e}^{\mathrm{j}k_{\mathrm{v}}h_1} + B_2 \mathrm{e}^{-\mathrm{j}k_{\mathrm{v}}h_1}}{A_1 \mathrm{e}^{\mathrm{j}k_{\mathrm{q}}h_1} + B_1 \mathrm{e}^{-\mathrm{j}k_{\mathrm{q}}h_1}} \tag{26}$$

Substituting the expression term of A_1, B_1, B_2 into the equation, the slip parameter can be expressed as

$$\alpha = \frac{G/\delta}{G/\delta + \rho_{\mathrm{l}} \Delta_{\mathrm{l}} \omega^2 + \mathrm{j}\hat{c}_{\mathrm{l}} k_{\mathrm{v}}} \tag{27}$$

From equation (27), the slip parameter can be calculated from the complex attraction strength value and the viscosity properties of the liquid environment. Inversely, the attraction strength between solid–liquid interfaces can be determined by measuring the slip parameter using a QCM, which will be discussed in the last section of this paper as an extensional application of the QCM.

3. Results and discussions

3.1. QCM impedance response in liquid with mechanical slip interface

With the parameters of the QCM as shown in table 1, the impedance spectrum of the unperturbed QCM can be obtained by setting the attraction strength $G^* = 0$ as in equation (22). The resonance frequency and anti-resonance frequency of the first thickness shear mode are 9.0032 MHz and 9.0233 MHz, respectively. Because the acoustic loss in the quartz crystal is extremely small, the impedance curve is considerably sharp as shown in figure 3. When the QCM is immersed into a viscoelastic liquid, its impedance spectrum sharpness is changed besides the resonance frequency shift. Under non-slip assumption, equation (24) can be used to determine the relationship between the viscosity of the liquid and the frequency shift as well as the Q-factor of the resonator. The amplitude and phase of the impedance and of the QCM in several kinds of liquid are computed as plotted in figures 4 and 5 with dotted lines. It can be seen from the figures that the Q-factor of the impedance spectrum is reduced significantly as the QCM is immersed into the liquid.

Based on the mechanical slip modelling, the response of the QCM in a viscoelastic liquid is affected by the contact condition of the interface. The amplitude and phase angle of the electrical impedance of the QCM results, evaluated from the mechanical slip model, with real attraction strength $G^* = 3000\,\mathrm{N\,m^{-2}}$, are presented in figures 4 and 5 with solid lines. For the numerical simulation, the interactive distance between atoms is set to be $\delta = 10^{-10}$ m. Compared with the results of the non-slip model, the series resonance frequency changes and changes in the Q-factor of the QCM are larger than

Table 1. Parameters for AT-cut QCM.

Quartz parameters	Value	Description
ρ_{q}	$2649\,\mathrm{kg\,m^{-3}}$	Density
c_{66}	$2.91 \times 10^{10}\,\mathrm{N\,m^{-2}}$	Shear modulus
e_{26}	$7.98 \times 10^{-2}\,\mathrm{C\,m^{-2}}$	Piezoelectric constant
ϵ_{22}	$3.982 \times 10^{-11}\,\mathrm{C\,V^{-1}\,m^{-1}}$	Permittivity
η_{q}	$8.376 \times 10^{-3}\,\mathrm{N\,s\,m^{-1}}$	Effective viscosity of quartz crystal
$\bar{A}$	$0.2984\,\mathrm{cm^2}$	Effective electrode surface area

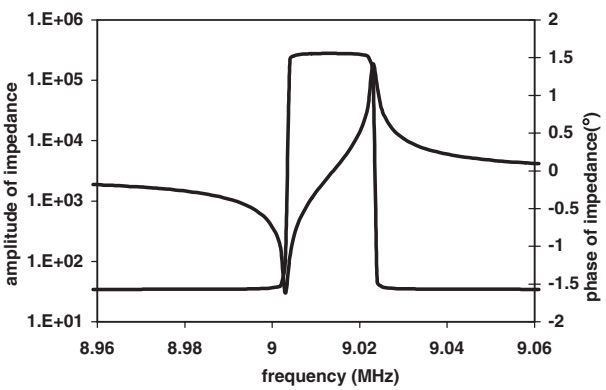

Figure 3. Impedance spectrum of the unperturbed QCM.

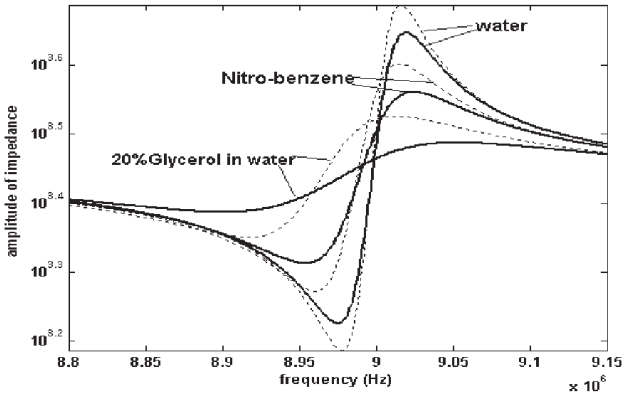

Figure 4. Amplitude of the impedance of the QCM in three kinds of liquid (· · · · · ·, non-slip modelling; ——, slip modelling).

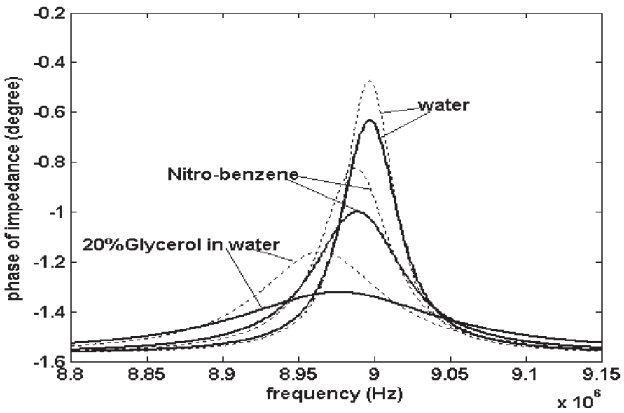

Figure 5. Phase angle of the impedance of the QCM in three kinds of liquid (· · · · · ·, non-slip modelling; ——, slip modelling).

Table 2. Results for series resonant frequency shift for immersion of one face of the QCM in a liquid.

			Frequency shift (kHz)	
Liquid	Density ($\mathrm{kg\,m^{-3}}$)	Viscosity ($\mathrm{N\,s\,m^{-2}}$)	Non-slip	Slip with $G^* = 3000\,\mathrm{N\,m^{-2}}$
Water	997	0.089	−25.2	−28.2
Nitro-benzene	1198.6	0.1811	−43.2	−49.2
20% glycerol in water	1025.2	0.7550	−86.2	−103.2

that evaluated from the corresponding non-slip mode when setting the attraction strength $G^* = 3000\,\mathrm{N\,m^{-2}}$ (table 2). The difference between these two models is that the inertia effect and phase changes between two contact interfaces are included in the mechanical slip modelling.

The sensitivity of the series resonant frequency and its impedance resonance amplitude to the viscosity of the liquid, η_v with differing attraction strength is plotted in figures 6 and 7, respectively. For the numerical simulation, the tiny shear storage of the liquid is set to be $\mu_\mathrm{l} = 10\,\mathrm{N\,m^{-2}}$ and the density of the liquid is kept constant, $\rho_\mathrm{l} = 1020\,\mathrm{kg\,m^{-3}}$. As the liquid viscosity increases, the energy dissipated into the liquid increases during each vibration cycle. The attraction strength at the solid–liquid interface transforms the vibration of the top surface of the quartz plate into the liquid medium. Different values of the attraction strength result in different

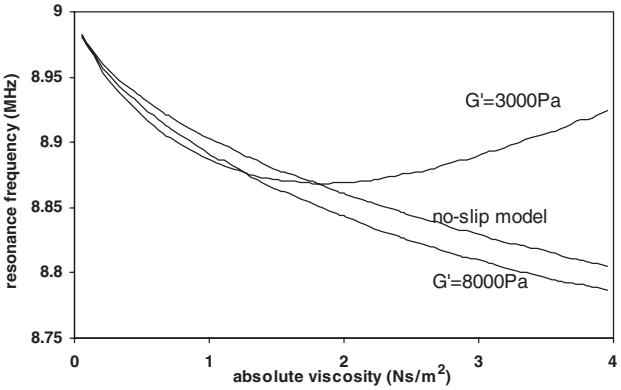

Figure 6. Series frequency of the compounded QCM as a function of the liquid viscosity.

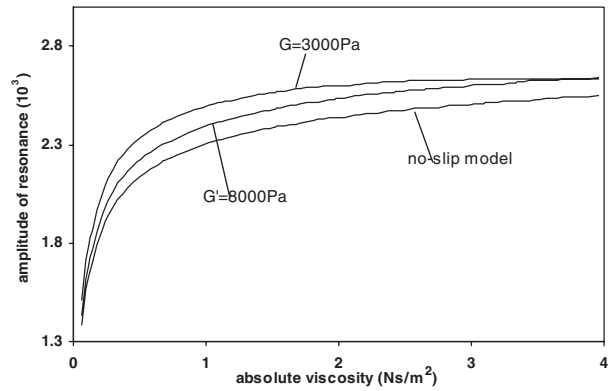

Figure 7. Amplitude of impedance at series resonance as a function of the liquid viscosity.

amounts of energy transformation. From the figures, it can be seen that when the QCM is subject to lower viscosity liquid loading, the frequency shift evaluated from the non-slip modelling is smaller than that evaluated from mechanical slip modelling. However, with a lower attraction strength, $G^* = 3000\,\mathrm{N\,m^{-2}}$, the resonance frequency is increased after the viscosity reaches a certain value and even higher than that of the unperturbed QCM. This is because the coupling of the viscosity and the interactive strength of the interface are considered. The response of the compounded QCM depends on the attraction strength when it is operating in the liquid environment. In the normal condition, when the interface attraction strength is higher than a critical value, the results evaluated from the mechanical slip modelling approaches that evaluated from non-slip modelling. It is an intuitive conclusion that when the attraction strength is infinitely large, there is no slip between the two interfaces, which is the same as the continuous displacement assumption.

3.2. Discussion on solid–liquid interfacial slip parameter

Ferrante [11] described the interfacial slip phenomenon of the compounded QCM in a liquid environment using a slip parameter, which was defined as the ratio between the particle displacement of the top surface of the quartz plate and that of the bottom surface of the liquid layer. From equation (27), the slip parameter is a function of the attraction strength as well as the properties of the bulk liquid. The distance between

the atomic particles is of the order of 10^{-10} m. The part of the mass inertia of the contact particles $\rho_l \Delta_l \omega^2$ is much smaller compared with the other two parts, G^*/δ and $j\hat{c_l}k_v$, with operating frequency at several megahertz. Neglecting the mass inertia of the liquid particles at the contact interface, the slip parameter can be rewritten as

$$\alpha = \frac{G^*/\delta}{G^*/\delta + j\omega\sqrt{\rho_l \hat{c_l}}} \tag{28}$$

Recalling the definition of the slip parameter, the relationship between the displacement of the liquid layer and the quartz crystal plate at the contact interface can be written as

$$u_l^h + \Re \dot{u}_l^h = u_q^h \tag{29}$$

where $\Re$ is a function of the contact interface properties and bulk liquid properties,

$$\Re = \frac{\delta\sqrt{\rho_l \hat{c_l}}}{G^*} \tag{30}$$

McHale [13] introduced a single parameter, s, to consider the slip boundary condition in his impedance analysis of the acoustic wave sensors in a liquid environment. Comparing equations (29) and (31) of [13], the parameter $\Re$ in this paper is the same as the parameter s proposed by McHale [13], in whose paper the parameter s is assumed to be a real parameter.

It is reasonable that the slip parameter has a certain relationship with the bulk liquid viscosities besides the contact interface itself. With the model proposed in this paper, the slip parameter, α [11], and s [13] are explored in greater detail for more physical meanings.

The contact attraction strength between two contact layers is a complex value; the physical concept can be illustrated with a spring and dashpot connected between the contact interfaces:

$$G^* = G' + j\omega G'' \tag{31}$$

The slip parameter is a function of the attraction strength and the bulk liquid viscosity. Figures 8 and 9 give the amplitude of the slip parameter, $|\alpha|$, and its phase as G' and the imaginary part, G'', are varied, in which the operating frequency $f = 8.98$ MHz, the bulk liquid viscosity is set at $\eta_l = 0.29\,\mathrm{N\,s\,m^{-2}}$, the interface distance is set as $\delta = 10^{-10}$ m and the density of the liquid $\rho_l = 1020\,\mathrm{kg\,m^{-3}}$. The attraction strength can be a complex value. As shown in figures 8 and 9, when the attraction strength goes to infinity, the slip parameter approaches 1. This is the maximal amplitude of the slip parameter when the imaginary part of the interactive strength is 0. As the interactive slip parameter goes to 0, the slip parameter approaches 0 as well. When the real part is set to be 0, the modelling is the same as in the friction model discussed in McHale's paper [13], that the interface force is related to the relative velocity of the contact layers with a friction coefficient. The slip parameter increases with increasing magnitude of the imaginary part of the interactive strength.

The slip parameter is not linearly proportional to the liquid viscosity. The changing trend of the amplitude of the slip parameter as a function of the liquid viscosity varies with varying interface attraction strength [14]. With zero imaginary

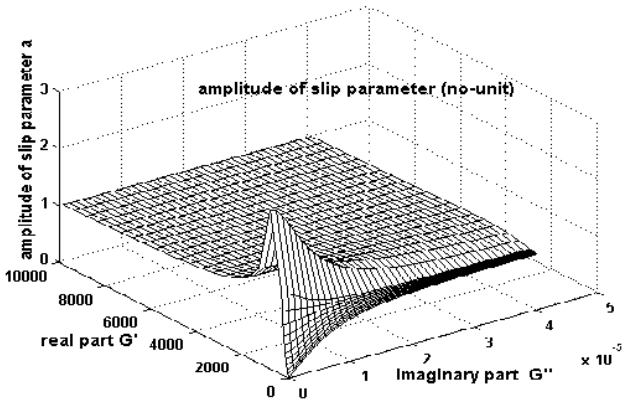

Figure 8. Amplitude of slip parameter as a function of the interactive strength, G', and G''.

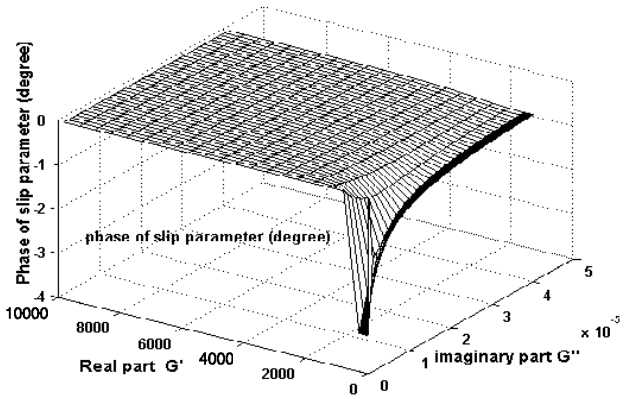

Figure 9. Phase of the slip parameter as a function of the interactive strength, G', and G''.

part of the attraction strength, i.e. $G'' = 0$, when the interactive strength is smaller than a value corresponding to the maximum amplitude of the slip parameter, the slip parameter decreases as the viscosity of the bulk liquid increases. However, for a higher interactive strength at the solid–liquid interface, the amplitude of the slip parameter increases as the viscosity of the bulk liquid increases.

3.3. Determine the solid–liquid interface interactive strength with the QCM

An insight into the slip parameter of the QCM operating in the liquid environment it might be used for a fresh application of the QCM, for example, to measure the attraction strength between the solid and liquid by measuring the slip parameter.

From equation (28), the attraction strength can be expressed as

$$\frac{G^*}{\delta} = \frac{j\alpha}{1-\alpha}\hat{c_l}k_v = \frac{\alpha}{1-\alpha}\omega\sqrt{-\rho_l \hat{c_l}} \tag{32}$$

where α is the slip parameter, which can be measured by experiments.

Using the experimental results from Ferrante [11] as listed in table 3, the attraction strength of a liquid of different viscosity to a hydrophilic-coated (using 1-mercapto undecanoic acid) sensor and a hydrophobic-coated (using 1-mercapto hexadecane) sensor used in that paper can be

Table 3. Interactive strength calculated from slip parameters from Ferrante's paper.

Glycerol in water			Hydrophilic-coated		Hydrophobic-coated	
Fraction	Density ($kg\,m^{-3}$)	Viscosity ($N\,s\,m^{-2}$)	α (no unit)	$\frac{G^*}{\delta}$ ($10^{14}\,N\,m^{-3}$)	$\lvert\alpha\rvert$ (phase) (no unit)	$\frac{G^*}{\delta}$ ($10^{14}\,N\,m^{-3}$)
0.0	1000.0	0.100 2	$4.419(31.35^0)$	$-0.031 - 0.042i$	$5.503(24.60^0)$	$-0.0324 - 0.0389i$
0.1	1012.6	0.290 32	$2.911(25.34^0)$	$-0.056 - 0.086i$	$3.501(21.03^0)$	$-0.0591 - 0.0783i$
0.2	1025.2	0.755 08	$2.022(18.79^0)$	$-0.101 - 0.187i$	$2.446(16.42^0)$	$-0.1072 - 0.1576i$
0.3	1037.8	1.761 20	$1.727(13.39^0)$	$-0.186 - 0.350i$		
0.4	1050.4	4.103 02	$1.447(8.461^0)$	$-0.383 - 0.745i$	$1.405(6.086^0)$	$-0.4682 - 0.7940i$
0.5	1063.1	7.168 15	$1.321(5.110^0)$	$-0.718 - 1.260i$		
0.6	1075.7	15.285 1	$1.174(3.393^0)$	$-0.1529 - 3.082i$	$1.176(0.142^0)$	$-2.5310 - 2.6032i$
0.7	1088.3	36.010 9	$0.937(1.000^0)$	$10.492 + 5.932i$		
0.8	1100.9	62.981 3	$0.893(-0.285^0)$	$6.267 + 6.878i$	$0.868(-2.855^0)$	$2.8325 + 6.3171i$
0.9	1113.5	109.846	$0.844(-3.234^0)$	$3.208 + 6.901i$		
1.0	1126.1	157.429	$0.832(-4/556^0)$	$2.679 + 7.659i$	$0.823(-8.202^0)$	$0.5205 + 6.6720i$

* The slip parameters α are taken from Ferrante's paper [11].

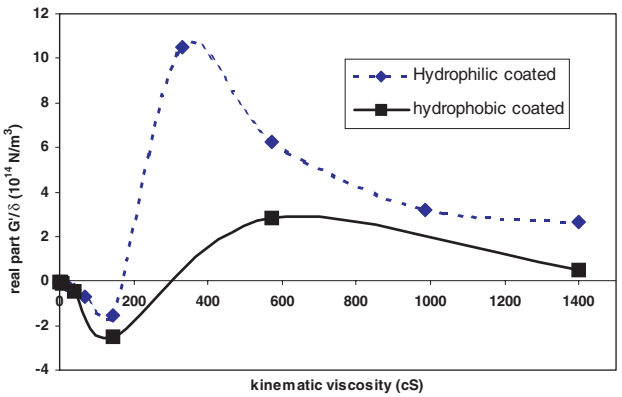

Figure 10. Real part of the interactive strength of the liquid–solid interface, G'/δ, as a function of the bulk liquid viscosity (calculated from experimental results of Ferrante [11]).

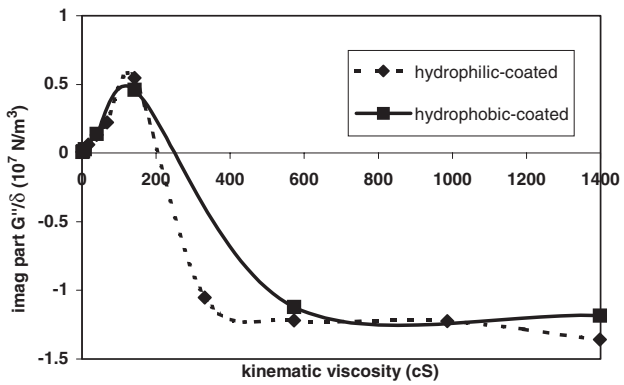

Figure 11. Imaginary part of the interactive strength of interface, G''/δ, as a function of bulk liquid viscosity (calculated from experimental results of Ferrante [11]).

calculated as listed in table 3. The real part of the attraction strength, G'/δ, and the imaginary part of the attraction strength, G''/δ, are plotted versus the kinematic viscosity of the liquid in figures 10 and 11, respectively.

When the viscosity of the liquid is lower (mole fraction is lower), the real part and the imaginary part of the interface attraction strength for hydrophilic-coated and hydrophobic-coated sensors are quite close. However, as the glycerol fraction increases (viscosity is higher), the hydrophilic-coated sensor (dotted line in figure) gives a higher attraction strength than the hydrophobic-coated sensor (solid line in figure). It is found that the imaginary parts of the interactive strengths of these two types of sensors are almost the same. The real part of the interactive strength of the hydrophilic-coated sensor is larger than that of the hydrophilic-coated sensor. This is not in conflict with the reality that the hydrophilic-coated surface has a larger attraction strength with the viscosity liquid. In addition, the imaginary part of the attraction strength for both types of sensor is reduced with an increased fraction of glycerol. From the results, it is shown that with a real friction coefficient (imaginary part interactive strength G'') alone as in McHale's paper [13] it is not enough to distinguish the different interface conditions for different types of sensor. The real part of the interactive strength contributes significantly to distinguish the different interface conditions for these two types of sensors.

Of course, it is not fair to draw a conclusion that the relationship between the viscosity of liquid and the solid–liquid interface attraction strength follows a simple curve as in this paper because the physical details of atomic attraction are much more complicated. The physical mechanism of the atomic attraction between glycerol and the coating materials used in Ferrante's experiment [11] has not been considered. However, the model presented in this paper is an attempt to evaluate the solid–liquid interface attraction strength using a QCM by measuring the slip parameter.

4. Conclusions

A continuous displacement assumption for a QCM in a liquid masks the physical details of the contact interface between the solid and liquid when the QCM operates in a liquid environment. In this paper, a mechanical slip model that involves the properties of the contact interface, such as interactive strength, contact molecular size and viscosity of the liquid, is discussed and used to describe the response of the QCM in a viscous liquid. The slip parameter is expressed explicitly as a function of the interface attraction strength of contact layers, G^*, and the viscosity of the liquid. The detailed mechanical description of the solid–liquid interface of the

QCM in a liquid provides a physical approach to understanding the performance of the QCM in a liquid.

The detailed physical description of the solid–liquid interface is useful for exploring the use of the QCM in the biological industry. With the mechanical slip model of the interface, a new approach by using the slip parameter measured with the QCM is proposed to determine the attraction strength between the particles of a viscous liquid and solid particles. The experimental data reported in the literature for a hydrophilic-coated sensor and a hydrophobic-coated sensor are used for the numerical examples. It is found that the imaginary parts of the interactive strength of two types of sensor are almost the same and the real parts of the interactive strength contribute significantly to distinguish the different interface conditions for these two types of sensor.

References

[1] Sauerbrey G 1959 Verwendung von schwingquarzen zur wagung dunner schechten and zur mikrowagung *Z. Phys.* **155** 206–22

[2] Nomura T and Okugara M 1982 Frequency shifts of piezoelectric quartz crystals immersed in organic liquids *Anal. Chim. Acta* **142** 281–4

[3] Cavic B A, Chu F L, Furtado L M, Ghafouri S, Hayward G L, Mack D P, McGovern M E, Su H and Thompson M 1997 Acoustic waves and the real-time study of biochemical macromolecules at the liquid/solid interface *Faraday Discuss.* **107** 159–76

[4] Rosler S, Lucklum R, Borngraber R, Hartmann J and Hauptmann P 1998 Sensor system for the detection of organic pollutants in water by thickness shear mode resonators *Sensors Actuators* B **48** 415–24

[5] Lucklum R, Behling C, Cernosek R W and Martin S J 1997 Determination of complex shear modulus with thickness shear mode resonators *J. Phys. D: Appl. Phys.* **30** 346–56

[6] Cernosek R W, Martin S J, Robert Hillman A and Bandey H L 1998 Comparison of lumped-element and transmission-line models for thickness-shear-mode quartz resonator sensors *IEEE Trans. Ultrasonics, Ferroelectrics Frequency Control* **45** 1399–407

[7] Miller J G and Bolef D I 1968 Sensitivity enhancement by the use of acoustic resonators in CW ultrasonic spectroscopy *J. Appl. Phys.* **39** 4589–93

[8] Lu C S and Lewis O 1972 Investigation of film-thickness determination by oscillating quartz resonators with large mass load *J. Appl. Phys.* **43** 4385–90

[9] Reed C E, Kanazawa K K and Kaufman J H 1990 Physical description of a viscoelastically loaded AT-cut quartz resonator *J. Appl. Phys.* **68** 1993–2001

[10] Kanazawa K K 1997 Mechanical of films on the quartz microbalance *Faraday Discuss.* **107** 77–90

[11] Ferrante F, Kipling A L and Thompson M 1994 Molecular slip at the solid–liquid interface of an acoustic-wave sensor *J. Appl. Phys.* **76** 3448–62

[12] Rodahl M and Kasemo B 1996 On the measurement of thin liquid overlayers with the quartz-crystal microbalance *Sensors Actuators* A **54** 448–56

[13] McHale G, Lucklum R, Newton M I and Cowen J A 2000 Influence of viscoelasticity and interfacial slip on acoustic wave sensors *J. Appl. Phys.* **88** 7304–12

[14] Lu F, Lee H P and Lim S P 2003 Mechanical description of interfacial slips for quartz crystal microbalances with viscoelastic liquid loading *Smart Mater. Struct.* **12** 881–8

[15] Ballantine D S Jr, White R M, Martin S J, Ricco A J, Frye G C, Zellers E T and Wohltjen H 1997 *Acoustic Wave Sensors: Theory, Design and Physico-Chemical Application* (New York: Academic)